



# Relationship between steady-state and induced gamma activity to motion

Giri P. Krishnan,<sup>CA</sup> Patrick D. Skosnik, Jenifer L. Vohs, Thomas A. Busey and Brian F. O'Donnell

Department of Psychology, Indiana University, Bloomington, IN 47405, USA

<sup>CA</sup>Corresponding Author: gpkrishn@indiana.edu

Received 17 January 2005; accepted 10 February 2005

When a moving stimulus is presented at a specific temporal frequency, both steady-state responses and induced  $\gamma$  activity may be elicited in the electroencephalogram. The electroencephalogram was recorded when study participants viewed random dot kinematograms under three conditions: coherent motion, incoherent motion and stationary. Dot position was changed at a rate of 9.3 Hz in the coherent and incoherent conditions. Induced power at

40 Hz was increased during coherent motion compared with the other conditions. In contrast, the steady-state response at 9.3 Hz showed a trend for increased power during the incoherent condition. These results suggest that steady-state responses to moving stimuli reflect sensory activation, while the induced  $\gamma$  activity indexes perceptual processes. *NeuroReport* 00:000–000 © 2005 Lippincott Williams & Wilkins.

**Key words:** Electroencephalogram; Induced  $\gamma$  activity; Motion; Random dot kinematograms; Steady-state activity

## BACKGROUND

Visual features such as motion, spatial frequency and color are processed by distributed neural circuits [1,2]. The visual perception of objects in space therefore requires binding multiple features to form a single percept. Synchronization in firing of different regions of the brain may be a mechanism facilitating the binding process [3–5]. When such synchronization occurs, the firing rate of neurons usually centers within the  $\gamma$  range (30–100 Hz) [6,7].

In humans, the electroencephalogram (EEG) has been used to investigate the relationship between neural synchronization and perception. Several studies have shown enhancement of  $\gamma$  activity in the EEG during visual tasks when coherent representations are generated e.g. [8]. Induced  $\gamma$  activity has also been observed in intracranial recordings in humans using a similar visual paradigm [9]. Previous studies have demonstrated that coherently moving bars, but not incoherent motion, produced a burst of  $\gamma$  activity during passive viewing [10,11]. Thus,  $\gamma$  activity in EEG occurs with stimuli and in conditions similar to those that elicit synchronization at the cellular level.

The EEG may also be entrained by periodic stimulation. When a temporally modulated visual stimulus is presented, the EEG shows phase-locked oscillations at the stimulus frequency. This entrainment of the EEG has been referred to as the steady-state response, and can be elicited by both flickering and moving stimuli [12,13].

Both steady-state and induced  $\gamma$  activity have been used to study visual processing. However, it is not clear whether these two types of oscillations reflect the activity of the same or different neural circuits or how they relate to perceptual processes. One approach to this question is to determine whether varying stimulus features affect the two types of

responses differentially. We used this technique to identify the neural correlates of steady-state and induced  $\gamma$  activity to motion. A random dot kinetogram (RDK) was used to elicit both steady-state and induced  $\gamma$  activity to motion. The periodic changes of the position of the dots in RDK evoke a steady-state potential at the frequency of displacement [13]. Because the perception of global motion in RDK requires integration of local motion signals [14], we hypothesized that a coherent RDK would induce  $\gamma$  activity, as has been shown in animal studies [15,16], while the incoherent RDK would not.

## METHOD

Seventeen healthy study participants (nine women, age=23.2±2.9 years) took part in this experiment. An informed written consent was obtained. Participants were asked to relax, keep their eyes open and focus on the display during stimulus presentation. All stimuli were presented on a Power Macintosh computer. The experiment included three conditions: coherent motion, incoherent motion and stationary. In the coherent condition, all dots in RDK were displaced from left to right within the stimuli window, and during the incoherent condition, all dots were displaced at randomly generated angles. The dots were static in the stationary condition. A total of 100 dots were used to generate the RDK. The stimulus window subtended 5° of the visual angle and the rate of displacement of dots was 5°/s. The position of dots was refreshed every 107.5 ms (9.3 Hz) for both the coherent and incoherent conditions. All trials were presented for 1600 ms, with a 1.5-s interval between trials. There were 100 trials in all three conditions. However, eight participants had only 50 trials in the

stationary condition. The conditions were randomized across trials and participants were given breaks after every 50 trials. EEG was recorded with a sampling rate of 1000 Hz and filtered between 1 and 200 Hz. EEG was recorded from 14 scalp electrodes using an electrode cap and additional electrodes to record the vertical and horizontal electrooculogram. The electrode impedance was maintained below 10 k $\Omega$ . All channels were referenced to the right ear lobe.

The recorded EEG was segmented into trials that began at stimulus onset and ended at 1600 ms. Trials that had amplitude values exceeding  $\pm 100 \mu\text{V}$  were rejected from further processing. Eye movement artifact was corrected using Gratton's algorithm [17]. The steady-state potentials were obtained for the time period when the stimulus was presented after averaging across trials within each condition. A fast Fourier transform (FFT) was used to obtain the power spectrum from the averaged event-related potential. The  $\log_{10}$  power at 9.3 Hz was calculated at Pz and Oz for statistical analysis. The Vision Analyzer was used for EEG analysis (Brain Products, GmbH, München, Germany).

Induced  $\gamma$  activity was measured using a wavelet-based time frequency transform. A Morlet wavelet with a wavelet factor of 8 was convoluted with the single trials. The resultant transformation had 35 frequency steps between 10 and 70 Hz with varying frequency resolution for every time point. The time frequency transforms from single trials were averaged. The averaged transform was used for statistical analyses. A baseline subtraction was then computed using

the average power in the interval 500 ms before the stimulus onset at each frequency.

For statistical analysis, power values from the  $\gamma$  band range (frequency bins with center frequencies ranging from 40 to 60 Hz) were averaged using sequential 100-ms windows between onset and offset of the stimuli (1600 ms). This resulted in 16 power values for every participant and every channel, which were then  $\log_{10}$  transformed for statistical analysis. Data from Cz, Pz and Oz were used for analysis of induced  $\gamma$ , and Pz and Oz for steady-state activity, because the responses were largest at these electrode sites. Because our primary objective was to compare the coherent and incoherent conditions, a repeated measure ANOVA was calculated for these two conditions with the factors channels (2 or 3) and time (16). Similar ANOVAs were also computed to compare the coherent with static and incoherent with static conditions. A one-way ANOVA was used to identify the time periods when a time by condition interaction was significant. Greenhouse-Geisser-corrected significance values were used wherever applicable.

The time frequency transform of the coherent condition suggested that the  $\gamma$  power oscillated during stimulus presentation. In order to identify the frequency at which  $\gamma$  activity changed over time, an FFT was computed on the power of  $\gamma$  frequency bin (center frequency of 50 Hz) derived from the wavelet analysis for time period between 0 and 1600 ms.

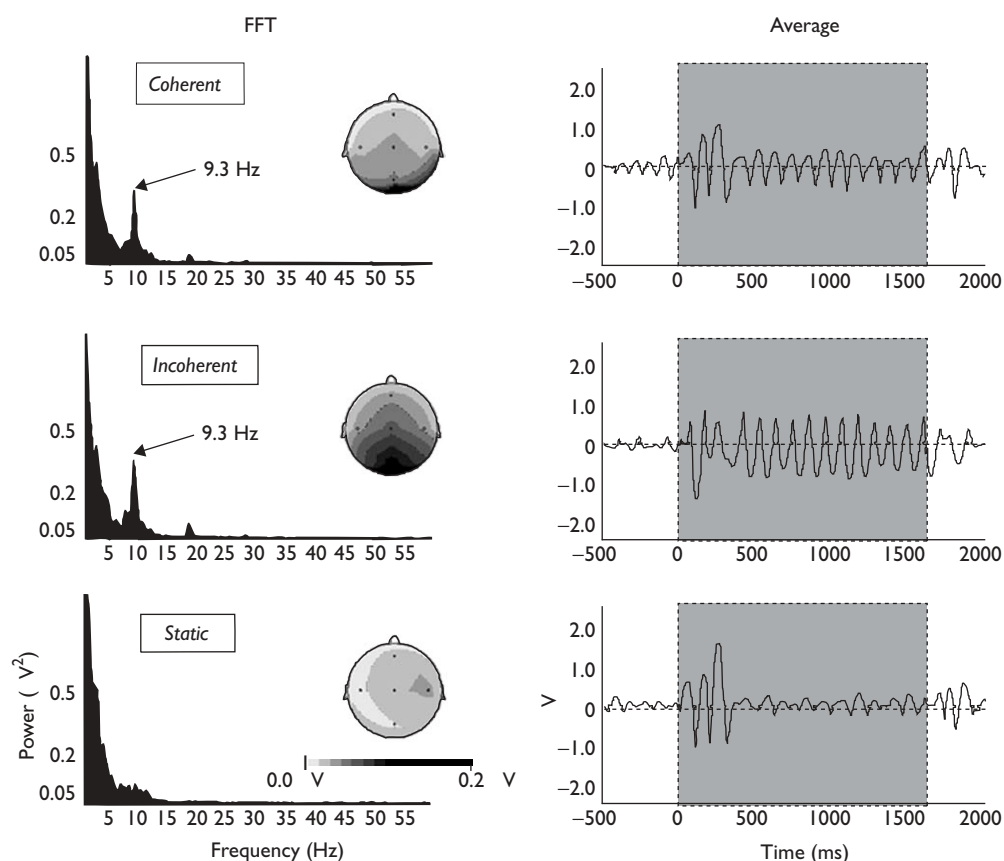


**Fig. 1.** Averaged waveforms and power spectra (for Oz) and spatial distribution of the steady-state response at 9.3 Hz for three conditions. The waveforms were filtered between 8 and 12 Hz before averaging across participants.

**RESULTS**

Figure 1 shows the averaged steady-state potential, averaged power spectrum and spatial plot of power at 9.3 Hz to three conditions. In both the coherent and incoherent conditions, the steady-state potentials were larger in the posterior head regions (Oz and Pz). The ANOVA on power at 9.3 Hz from the two electrode sites (Pz and Oz) showed a trend for increased activity during the incoherent condition [F(1,32)=3.67,  $p=0.06$ ]. The channel effect for this comparison was significant [F(1,32)=9.46,  $p<0.01$ ] with Oz having the highest amplitude.

The wavelet-based time frequency analysis showed bursts of  $\gamma$  activity centered around 40 Hz during the coherent motion condition, but not during the other conditions (Fig. 2a). Figure 2b shows the average spatial distribution across participants during three different duration segments of 100 ms in the  $\gamma$  frequency band (frequency bins with center frequency ranging from 40 to 60 Hz). The spatial distribution showed maximum  $\gamma$  activity at the central and parietal regions around 500 ms after the onset of the stimuli and continued until 1400 ms. The  $\gamma$  band activity was higher at

all the electrode sites during the coherent condition compared with the incoherent and static conditions.

The ANOVA comparing the coherent with incoherent conditions showed main effects for condition [F(1,32)=14.74,  $p<0.01$ ], time [F(15,480)=4.58,  $p<0.01$ ], channel [F(2,64)=7.99,  $p<0.01$ ] and a time by condition interaction [F(15,480)=4.62,  $p<0.01$ ]. A one-way ANOVA at every time point was used to characterize the time by condition interaction. This analysis showed that the power at  $\gamma$  frequency differed between coherent and incoherent conditions from 500 to 1600 ms (Fig. 3). The ANOVA comparing the coherent with static conditions also showed main effects for condition [F(1,32)=4.45,  $p<0.05$ ], time [F(15,480)=5.21,  $p<0.01$ ] and channel [F(2,64)=8.95,  $p<0.01$ ]. A significant time by condition effect [F(15,480)=2.16,  $p=0.05$ ] was displayed. In contrast, the ANOVA comparing the incoherent with static conditions showed no difference between conditions [F(1,32)=2.71,  $p=0.11$ ]. Only the effect of time [F(15,480)=3.30,  $p<0.01$ ] was significant.

The induced  $\gamma$  activity during the coherent condition showed an oscillatory modulation (Fig. 2a). An FFT was computed on the power values obtained from the time

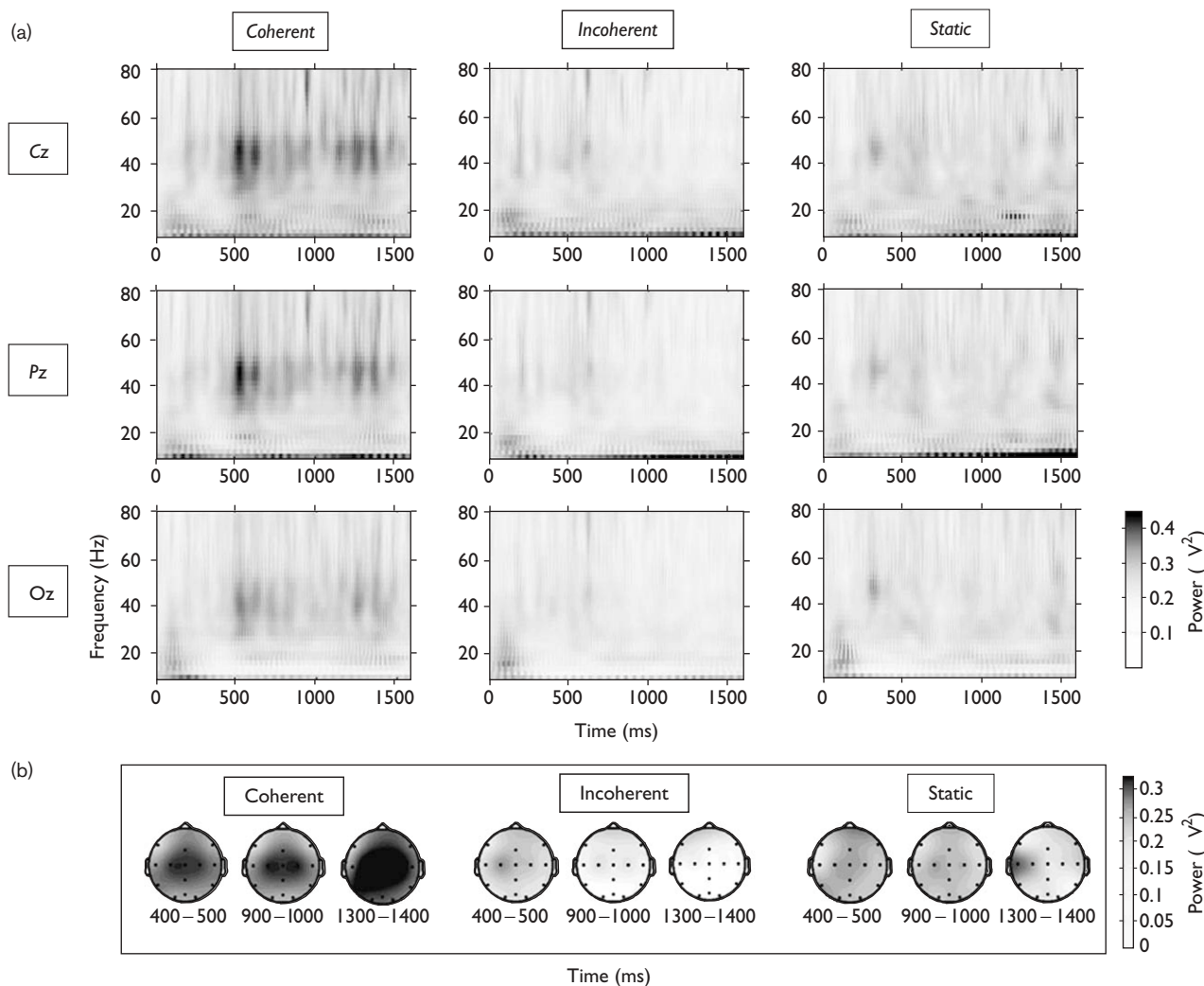


**Fig. 2.** (a) Average time frequency transform for the three conditions at Cz, Pz and Oz. (b) Average spatial distribution of power at  $\gamma$  frequency band (frequency bins with center frequency ranging from 40 to 60 Hz) during three different durations.

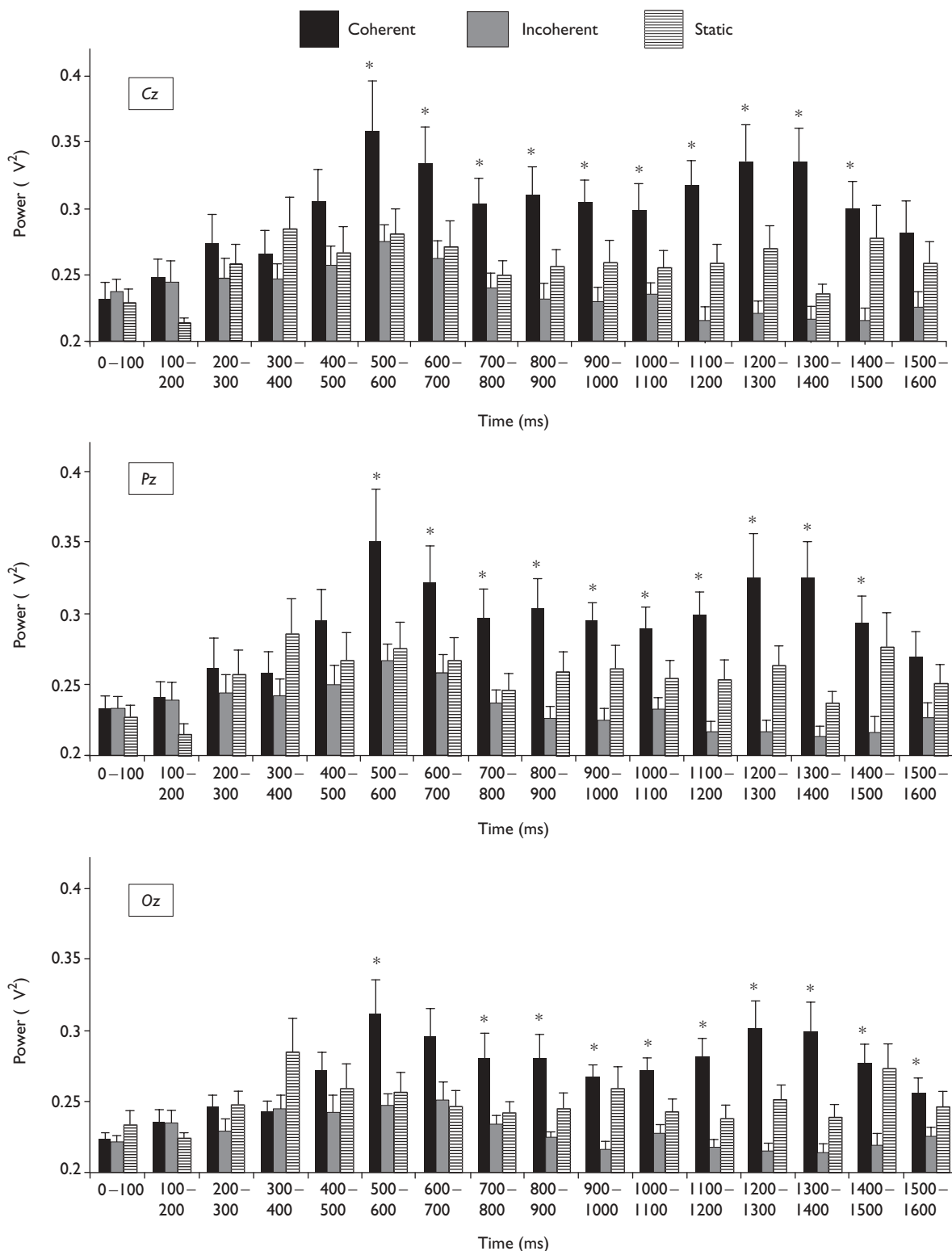


**Fig. 3.** Average  $\gamma$  band power at 100 ms intervals from Cz, Pz and Oz. The asterisk indicates a significant difference between the coherent and incoherent conditions. Error bars indicate standard errors.

frequency transform, which had a center frequency of 50 Hz from Cz. This showed a peak at 9.3 Hz in the averaged FFT across participants (Fig. 4). A similar analysis on the incoherent and static conditions did not show a peak at

this frequency (Fig. 4). Paired *t*-tests on the log value of the power at 9.3 Hz from this power spectrum showed significant differences between the coherent and incoherent conditions ( $t=2.54$ ,  $df=16$ ,  $p=0.02$ ).

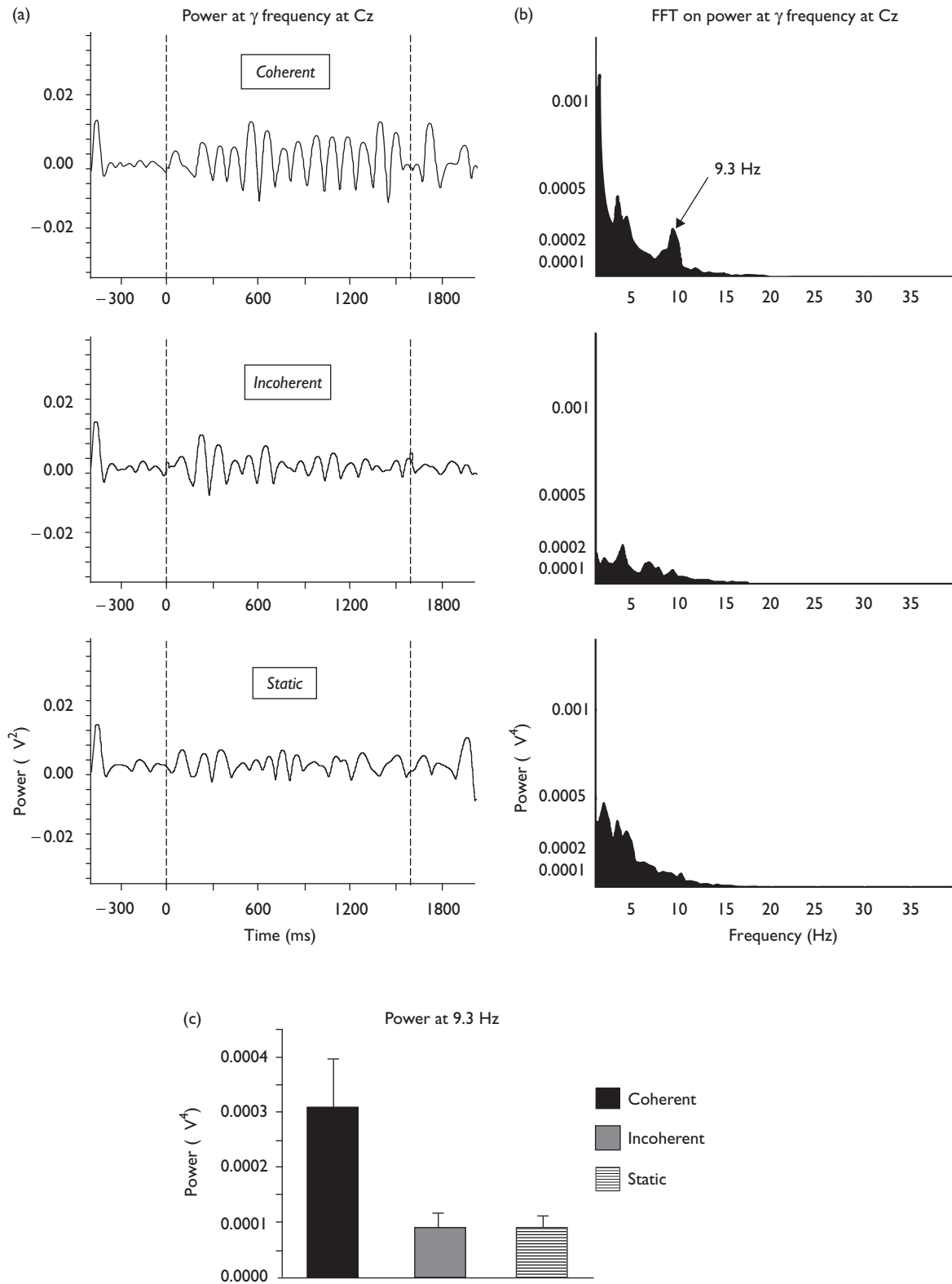


**Fig. 4.** (a) Average power at  $\gamma$  frequency (center frequency: 50 Hz) at Cz for every time point (obtained from the wavelet transform) for the three conditions. The waveforms were filtered between 8 and 12 Hz before averaging across participants. (b) Average fast Fourier transform (FFT) of the power at  $\gamma$  frequency (center frequency: 50 Hz) across participants (obtained from the wavelet transform). (c) Average power at 9.3 Hz from FFT of the power at  $\gamma$  frequency from three conditions. Error bars indicate standard error.

## DISCUSSION

The present study indicated that the coherent RDK elicited induced  $\gamma$  activity in the EEG, while incoherent motion or an array of stationary dots did not. Similar findings have been reported for moving bar stimuli [10] and for a kinetogram using magnetoencephalography [18]. These findings suggest that  $\gamma$  activity is generated during motion perception, and may reflect integration of information from multiple brain areas. Induced  $\gamma$  activity peaked approximately 500 ms after the onset of the stimulus. Similar latencies have been observed using moving bar stimuli, in which  $\gamma$  activity occurs between 300 and 500 ms after stimulus onset [10]. This period may reflect the bottom-up processes involved in object representation, and the time required to integrate motion information across a surface. The spatial distribution of the induced  $\gamma$  activity in this study showed a maximum at central and parietal electrode sites.

Steady-state-evoked potentials, in contrast to the induced  $\gamma$  activity, showed a trend for higher power during incoherent conditions compared with coherent conditions. The steady-state activity was present during the entire duration of the stimulus presentation, and had higher activity in the occipital regions (Fig. 1). Because the steady-state activity was generated for the entire duration of both coherent and incoherent motion, it may reflect the sensory activation to motion. Because induced  $\gamma$  activity was present only during coherent motion, it may be associated with perceptual processes [19].

The differences between steady-state and induced oscillations suggest that these responses have different neural sources. Primate studies have indicated that middle temporal (MT) is influenced by the coherence of the moving stimuli but that V1 activity is unaltered by coherence [20]. Moreover, a V1 neuron responds to its preferred motion irrespective of other motion vectors within its receptive field. In contrast, the responses of an MT neuron are reduced if motion vectors with different directions are present in its receptive field [21]. Therefore, it is likely that population response will increase in V1 and decrease in MT with increased incoherence. Consistent with this possibility, functional magnetic resonance image activation in MT+, but not V1, was shown to be proportional to the coherence of the stimuli [22,23]. With respect to the present data, steady-state responses may be generated in part by V1, while MT+ may act in concert with other cortical regions in the generation of the induced  $\gamma$  activity. However, sources of scalp activity cannot be directly identified solely on the basis of the EEG data, and further studies are required to identify sources at the cellular level.

Finally, this study showed that induced  $\gamma$  activity was modulated at the same frequency as the stimulus presentation. This suggests that the burst of  $\gamma$  activity occurs for each displacement of the coherent motion. If  $\gamma$  activity indexes the synchronization between different brain regions, then this finding suggests that perception of coherent motion involves synchronization in motion processing areas at every change of position of the dots in the RDK.

## CONCLUSION

This study indicated that induced  $\gamma$  activity was greater for coherent motion compared with incoherent motion or

stationary stimuli. Steady-state potentials, in contrast, were greater for incoherent motion compared with coherent motion. The findings from this study support the hypothesis that induced  $\gamma$  activity reflects perceptual processes such as object representation, while steady-state potentials may index early sensory activation.

## REFERENCES

- Zeki SM. Functional specialisation in the visual cortex of the rhesus monkey. *Nature* 1978; **274**:423–428.
- van Essen DC, Anderson CH, Felleman DJ. Information processing in the primate visual system: an integrated systems perspective. *Science* 1992; **255**:419–423.
- Singer W. Neuronal synchrony: a versatile code for the definition of relations? *Neuron* 1999; **24**:49–65.
- von der Malsburg C. The what and why of binding: the modeler's perspective. *Neuron* 1999; **24**:95–104.
- Engel AK, Roelfsema PR, Fries P, Brecht M, Singer W. Role of the temporal domain for response selection and perceptual binding. *Cereb Cortex* 1997; **7**:571–582.
- Gray CM, Viana Di Prisco G. Stimulus-dependent neuronal oscillations and local synchronization in striate cortex of the alert cat. *J Neurosci* 1997; **17**:3239–3253.
- König P, Engel AK, Singer W. Relation between oscillatory activity and long-range synchronization in cat visual cortex. *Proc Natl Acad Sci USA* 1995; **92**:290–294.
- Tallon-Baudry C, Bertrand O, Delpuech C, Pernier J. Stimulus specificity of phase-locked and non-phase-locked 40 Hz visual responses in human. *J Neurosci* 1996; **16**:4240–4249.
- Lachaux JP, Rodriguez E, Martinerie J, Adam C, Hasboun D, Varela FJ. A quantitative study of gamma-band activity in human intracranial recordings triggered by visual stimuli. *Eur J Neurosci* 2000; **12**:2608–2622.
- Müller MM, Junghöfer M, Elbert T, Rothstroh B. Visually induced gamma-band responses to coherent and incoherent motion: a replication study. *Neuroreport* 1997; **8**:2575–2579.
- Lutzenberger W, Pulvermüller F, Elbert T, Birbaumer N. Visual stimulation alters local 40-Hz responses in humans: an EEG-study. *Neurosci Lett* 1995; **183**:39–42.
- Regan D. *Human Brain Electrophysiology: Evoked Potentials and Evoked Magnetic Fields in Science and Medicine*. New York: Elsevier Publishers; 1989.
- Snowden RJ, Ullrich D, Bach M. Isolation and characteristics of a steady-state visually-evoked potential in humans related to the motion of a stimulus. *Vision Res* 1995; **35**:1365–1373.
- Smith AT, Snowden RJ, Milne AB. Is global motion really based on spatial integration of local motion signals? *Vision Res* 1994; **34**:2425–2430.
- Brecht M, Goebel R, Singer W, Engel AK. Synchronization of visual responses in the superior colliculus of awake cats. *Neuroreport* 2001; **12**:43–47.
- Kruse W, Hoffmann KP. Fast gamma oscillations in areas MT and MST occur during visual stimulation, but not during visually guided manual tracking. *Exp Brain Res* 2002; **147**:360–373.
- Gratton G, Coles MG, Donchin E. A new method for off-line removal of ocular artifact. *Electroencephalogr Clin Neurophysiol* 1983; **55**:468–484.
- Siegel M, Donner TH, Oostenveld R, Fries P, Engel AK. *Dependency of high-frequency neuronal oscillations in human area MT+ on visual motion strength: an MEG study*. Program no. 935.4. Abstract Viewer/Itinerary Planner. Washington, DC: Society for Neuroscience; 2004.
- Bertrand O, Tallon-Baudry C. Oscillatory gamma activity in humans: a possible role for object representation. *Int J Psychophysiol* 2000; **38**:211–223.
- Snowden RJ, Treue S, Erickson RG, Andersen RA. The response of area MT and V1 neurons to transparent motion. *J Neurosci* 1991; **11**:2768–2785.
- Andersen RA. Neural mechanisms of visual motion perception in primates. *Neuron* 1997; **18**:865–872.
- Heeger DJ, Boynton GM, Demb JB, Seidemann E, Newsome WT. Motion opponency in visual cortex. *J Neurosci* 1999; **19**:7162–7174.
- Muckli L, Singer W, Zanella FE, Goebel R. Integration of multiple motion vectors over space: an fMRI study of transparent motion perception. *Neuroimage* 2002; **16**:843–856.

Acknowledgements: This research was supported by NIMH I ROI MH62150-01, I R21-MH71816 (BFO), NIMH T32 MHI7146 (JLV) and an Indiana University Program in Neural Science Fellowship (GPK).

AUTHOR QUERY FORM

**LIPPINCOTT  
WILLIAMS AND WILKINS**

**JOURNAL NAME**                    **WNR**

**3/1/05**

**ARTICLE NO:**                    **3007**

**QUERIES AND / OR REMARKS**

<b>Query No</b>	<b>Details Required</b>	<b>Authors Response</b>
	No queries	